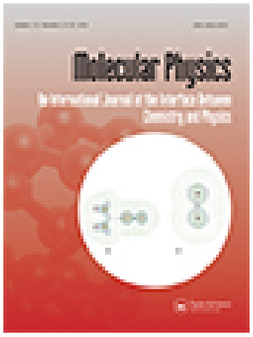

Taylor & Francis
Taylor & Francis Group

Molecular Physics

An International Journal at the Interface Between Chemistry and Physics

ISSN: 0026-8976 (Print) 1362-3028 (Online) Journal homepage: http://www.tandfonline.com/loi/tmph20

Effective potential method for active particles

Umberto Marini Bettolo Marconi, Matteo Paoluzzi & Claudio Maggi

To cite this article: Umberto Marini Bettolo Marconi, Matteo Paoluzzi & Claudio Maggi (2016): Effective potential method for active particles, Molecular Physics, DOI: 10.1080/00268976.2016.1155777

To link to this article: http://dx.doi.org/10.1080/00268976.2016.1155777

Published online: 11 Mar 2016.

MOLECULAR PHYSICS, 2016
http://dx.doi.org/10.1080/00268976.2016.1155777

Taylor & Francis
Taylor & Francis Group

SPECIAL ISSUE IN MEMORY OF YIPING TANG

Effective potential method for active particles

Umberto Marini Bettolo Marconi[a,b], Matteo Paoluzzi[c] and Claudio Maggi[d]

[a]Scuola di Scienze e Tecnologie, Università di Camerino, Camerino, Italy; [b]INFN Perugia, Perugia, Italy; [c]Department of Physics, Syracuse University, Syracuse, NY, USA; [d]Dipartimento di Fisica, Universita Sapienza, Rome, Italy

ABSTRACT

We investigate the steady-state properties of an active fluid modelled as an assembly of soft repulsive spheres subjected to Gaussian coloured noise. Such a noise captures one of the salient aspects of active particles, namely the persistence of their motion and determines a variety of novel features with respect to familiar passive fluids. We show that within the so-called multidimensional unified coloured noise approximation, recently introduced in the field of active matter, the model can be treated by methods similar to those employed in the study of standard molecular fluids. The system shows a tendency of the particles to aggregate even in the presence of purely repulsive forces because the combined action of coloured noise and interactions enhances the effective friction between nearby particles. We also discuss whether an effective two-body potential approach, which would allow to employ methods similar to those of density functional theory, is appropriate. The limits of such an approximation are discussed.

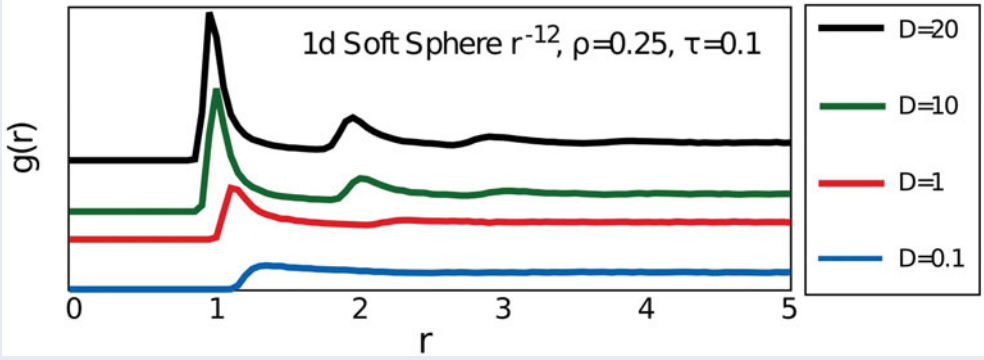

ARTICLE HISTORY
Received 30 November 2015
Accepted 10 February 2016

KEYWORDS
Active matter; non-equilibrium statistical mechanics; fluid structure of non-conventional fluids

1. Introduction

Recently, there has been an upsurge of interest towards the behaviour of the so-called active fluids whose elementary constituents are either self-propelled due their ability to convert energy into motion, for instance by chemical reactions, or receive the energy and impulse necessary to their motion when in contact with living matter, such as bacteria [1–6]. Examples of active matter systems include self-propelled colloids, swimming bacteria, biological motors, swimming fish and flocking birds. The phenomenology of active fluids is quite different from that characterising out-of-equilibrium molecular fluids, often referred as passive fluids, and for this reason the field is so fascinating. The theoretical studies are based on phenomenological models, constructed by using physical insight, with the aim to reproduce the complex biological mechanisms or chemical reactions determining the observed dynamics [7–10]. Among these models, we mention the important work of Cates, Tailleur and coworkers [11,12] who elaborated the Run-and-Tumble (RnT) model of Berg [13] and Schnitzer [14]. Such a model is based on the observations that the trajectories of individual bacteria consist of relatively straight segments (runs) alternated by erratic motions which cause the successive pieces of trajectory to be in almost random relative directions (tumbles). The persistence length of the trajectory sets the crossover between a ballistic regime at short time scales and a diffusive regime at longer times. Similarly, chemically propelled synthetic Janus colloids have a persistent propulsion direction which is gradually reoriented by Brownian fluctuations [15] (active Brownian particles).

CONTACT Umberto Marini Bettolo Marconi umberto.marinibettolo@unicam.it

Also, an ensemble of colloidal particles suspended in a 'bath' of such bacteria is a particular realisation of an active fluid [16–19]. Our description, at variance with the Cates and Tailleur model and the active Brownian model, involves only translational degrees of freedom of the particles, but not their orientations, and represents somehow a coarse-grained version of these models as also discussed by Farage et al. [20,21]. In the present model, in order to capture the peculiar character of the RnT motion on a coarse-grained time scales, one introduces a coloured noise, that is noise with a finite memory, which represents the persistence of the motion of the bacteria.

The observed behaviour displays a relevant feature: the particles display a spontaneous tendency to aggregate even in the absence of mutual attractive forces, as a result of the combined effect of coloured noise and interactions. This is a dynamic mechanism leading to a decrease of the particle effective mobility when the density increases.

Clearly, this behaviour cannot be described by standard equilibrium statistical mechanics, but it is possible to make progress in our understanding by applying kinetic methods and the theory of stochastic processes [22].

This paper is organised as follows. In Section 2, we present the coarse-grained stochastic model describing an assembly of active particles, consisting of a set of coupled Langevin equations for the coordinates of the particles subject to coloured Gaussian noise. After switching from the Langevin description to the corresponding Fokker–Planck equation, we obtain the stationary joint probability distribution of N particles within the multidimensional unified coloured noise approximation (MUCNA) [23–26]. The resulting configurational distribution function can be written explicitly for a vast class of inter-particle potentials and shows the presence of non-pairwise effective interactions due to the coupling between direct forces and the coloured noise. To reduce the complexity of the problem, in Section 3, we discuss whether it is possible to further simplify the theoretical study by introducing a pairwise effective potential. We analyse such an issue analytically by means of a system of just two particles in an external field and numerically using a one-dimensional system of N soft repulsive spheres. Our results show the limits of the effective two-body potential method. Finally, in the last section, we present our conclusions. Two appendices are included: in Appendix 1, we derive the UCNA approximation by means of multiple time-scale analysis and in Appendix 2, we obtain the key approximation of the theory necessary to evaluate the functional determinant of the MUCNA in the case of a many-particle system.

2. Model system

In this section, we briefly describe the salient assumptions employed to formulate the model adopted in the present work. First, consider an assembly of N overdamped active Brownian particles at positions $\mathbf{r}_i$, self-propelling with constant velocity v_0 along orientations $\boldsymbol{n}_i$, which change in time according to the stochastic law

$$\dot{\boldsymbol{n}}_i = \sqrt{D_r}\boldsymbol{\eta}_i \times \boldsymbol{n}_i \tag{1}$$

where $\boldsymbol{\eta}_i(t)$ are Gaussian random processes distributed with zero mean, time-correlations $\langle \boldsymbol{\eta}_i(t)\boldsymbol{\eta}_j(t')\rangle = 2\mathbf{1}\delta_{ij}\delta(t-t')$, and $D_r = 1/\tau$ is a rotational diffusion coefficient. In addition, the particles experience deterministic forces $\boldsymbol{F}_i = -\nabla_i \mathcal{U}$, generated by the potential energy $\mathcal{U}$. The resulting governing equations are

$$\dot{\mathbf{r}}_i = v_0\,\boldsymbol{n}_i + \gamma^{-1}\boldsymbol{F}_i, \tag{2}$$

where γ is the friction coefficient. The resulting dynamics are persistent on short time scales, i.e. the trajectories maintain their orientation for an average time τ, and diffusive on larger time scales. Hydrodynamic interactions are disregarded for the sake of simplicity together with inertial effects because particles are typically in a low-Reynolds-number regime [27].

Equations (1) and (2) involve the dynamics of both translational and rotational degrees of freedom and are not a practical starting point for developing a microscopic theory. Hence, it is convenient to switch to a coarse-grained description stochastically equivalent to the original one on times larger than τ . To this purpose, one integrates out the angular coordinates as shown by Farage *et al.* [20]. According to this approximation, one introduces a coloured stochastic noise term acting on the position coordinates and replacing the stochastic rotational dynamics (1). The effective evolution equations are

$$\dot{\mathbf{r}}_i(t) = \frac{1}{\gamma}\boldsymbol{F}_i(t) + \boldsymbol{u}_i(t), \tag{3}$$

with

$$\dot{\boldsymbol{u}}_i(t) = -\frac{1}{\tau}\boldsymbol{u}_i(t) + \frac{D^{1/2}}{\tau}\boldsymbol{\eta}_i(t), \tag{4}$$

where $\boldsymbol{u}_i(t)$ is an Ornstein–Uhlenbeck process with zero mean, time-correlation function given by

$$\langle \boldsymbol{u}_i(t)\,\boldsymbol{u}_j(t')\rangle = \frac{D}{\tau}e^{-2|t-t'|/\tau}\mathbf{1}\delta_{ij}. \tag{5}$$

and whose diffusion coefficient D is related to the original parameters by $D = v_0^2\tau/6$. In order to derive an equation

involving only the positions of the particles, we differentiate with respect to time (Equation (3)), and with simple manipulations, we get the following second-order differential equation:

$$\ddot{x}_i = \frac{1}{\gamma}\sum_k \frac{\partial F_i}{\partial x_k}\dot{x}_k - \frac{1}{\tau}\left[\dot{x}_i - \frac{F_i}{\gamma}\right] + \frac{D^{1/2}}{\tau}\eta_i(t), \quad (6)$$

where, for the sake of notational economy, we indicated by x_i the array $\{\mathbf{r}_i\}$ and similarly the components of the force. By performing an adiabatic approximation (see Appendix 1), we neglect the terms $\ddot{x}_i$ and obtain the following set of Langevin equations for the particles coordinates:

$$\dot{x}_i \simeq \sum_k \Gamma_{ik}^{-1}\left[\frac{1}{\gamma}F_k + D^{1/2}\eta_k(t)\right] \quad (7)$$

with the non-dimensional friction matrix Γ_{ik} defined as

$$\Gamma_{ik}(x_1, \ldots, x_N) = \delta_{ik} + \frac{\tau}{\gamma}\frac{\partial^2 \mathcal{U}(x_1, \ldots, x_N)}{\partial x_i \partial x_k}. \quad (8)$$

Note that, within the approximation introduced in Equation (7), the effective random force corresponds to a multiplicative noise due to its dependence on the state of the system, $x_i(t)$, through the prefactor $\Gamma_{ik}^{-1}(x_1, \ldots, x_N)$ in front of the noise term $\eta_k(t)$.

For the sake of concreteness, $\mathcal{U}$ is the sum of one-body and two-body contributions:

$$\mathcal{U}(x_1, \ldots, x_N) = \sum_i u(x_i) + \sum_{i>j} w(x_i, x_j). \quad (9)$$

The associated multidimensional Smoluchowski equation for the configurational distribution function associated with Equation (7) can be written as (see [21]):

$$\frac{\partial P_N(x_1, \ldots, x_N; t)}{\partial t} = -\sum_l \frac{\partial}{\partial x_l}\sum_k \Gamma_{lk}^{-1}\left(\frac{1}{\gamma}F_k P_N - D\sum_j \frac{\partial}{\partial x_j}[\Gamma_{jk}^{-1} P_N]\right) \quad (10)$$

and shows that the effective friction experienced by each particle also depends on the coordinates of all other particles. In order to determine the stationary properties of the model, we apply the following zero current condition in Equation (10) and get

$$-T_s\sum_\beta\sum_n \frac{\partial}{\partial r_{\beta n}}[\Gamma^{-1}_{\alpha l,\beta n}(\mathbf{r}_1, \ldots, \mathbf{r}_N)P_N(\mathbf{r}_1, \ldots, \mathbf{r}_N)] = P_N(\mathbf{r}_1, \ldots, \mathbf{r}_N)\left(\frac{\partial u(\mathbf{r}_{\alpha l})}{\partial r_{\alpha l}} + \sum_{k\neq l}\frac{\partial w(\mathbf{r}_l - \mathbf{r}_k)}{\partial r_{\alpha l}}\right) \quad (11)$$

The resulting stationary distribution can be written explicitly as (see [25]):

$$P_N(x_1, \ldots, x_N) = \frac{1}{Z_N}\exp\left(-\frac{\mathcal{H}(x_1, \ldots, x_N)}{T_s}\right), \quad (12)$$

where we have defined the effective temperature $T_s = D\gamma$ and the effective configurational energy of the system $\mathcal{H}(x_1, \ldots, x_N)$ related to the bare potential energy $\mathcal{U}(x_1, \ldots, x_N)$ by

$$\mathcal{H}(x_1, \ldots, x_N) = \mathcal{U}(x_1, \ldots, x_N) + \frac{\tau}{2\gamma}\sum_k^N\left(\frac{\partial \mathcal{U}(x_1, \ldots, x_N)}{\partial x_k}\right)^2 - T_s \ln|\det \Gamma_{ik}|, \quad (13)$$

where Z_N is a normalisation constant

$$Z_N = \mathrm{Tr}\exp\left[-\frac{\mathcal{H}(\mathbf{r}_1, \ldots, \mathbf{r}_N)}{T_s}\right]. \quad (14)$$

with $\mathrm{Tr} \equiv \int d\mathbf{r}_1, \ldots, d\mathbf{r}_N$. Formula (12) gives within the unified coloured noise approximation, a complete information about the configurational state of a system of N particles, but it requires the evaluation of a $dN \times dN$ determinant stemming from the matrix Γ_{ik}, where d is the dimensionality of the system. One can only get analytic results either by considering non-interacting systems with $d = 1, \ldots, 3$ or systems with few particles, where the computation of the determinant is possible. Thus, in spite of the fact that, in principle, from the knowledge of P_N, it is possible to determine all steady properties of the system, including the pair correlation function of the model, $g(\mathbf{r}_1, \mathbf{r}_2)$, this task is not possible in practice. The same situation occurs in equilibrium statistical mechanics, where from the knowledge of the canonical Boltzmann distribution of an N particle system, we cannot, in general, exactly determine the n-particle distribution functions with $n < N$. On the other hand, it is possible to derive a structure similar to the Born–Bogolubov–Green–Yvon (BBGY) hierarchy of equations linking the n-th order distribution to those of higher order, but it requires the specification of a closure relation. To this purpose, we integrate Equation (11) over $d(N-n)$ coordinates and obtain an equation for the marginalised probability distributions

of n particles, $P_N^{(n)}(\mathbf{r}_1, \ldots, \mathbf{r}_n)$ in terms of higher order marginal distributions. When $n = 1$, we find

$$T_s \int\int d\mathbf{r}_2 \ldots d\mathbf{r}_N \sum_{\beta=1}^{d}\sum_{n=1}^{N} \frac{\partial}{\partial r_{\beta n}} \times [\Gamma^{-1}_{\alpha 1,\beta n}(\mathbf{r}_1, \ldots, \mathbf{r}_N) P_N(\mathbf{r}_1, \ldots, \mathbf{r}_N)] = -P_N^{(1)}(\mathbf{r}_1)\frac{\partial u(\mathbf{r}_1)}{\partial r_{\alpha 1}} - (N-1) \times \int d\mathbf{r}_2 P_N^{(2)}(\mathbf{r}_1, \mathbf{r}_2)\frac{\partial w(\mathbf{r}_1 - \mathbf{r}_2)}{\partial r_{\alpha 1}}, \tag{15}$$

where Greek indexes stand for Cartesian components.

In the case of a large number of particles, the exact matrix inversion necessary to use formula (15) becomes prohibitive. However, we notice that in the limit of small (τ/γ) and $N \to \infty$, the structure of the matrix $\Gamma^{-1}_{\alpha 1,\beta n}$ becomes much simpler as illustrated in Appendix 2, and can be approximated by

$$\Gamma^{-1}_{\alpha l,\beta n}(\mathbf{r}_l) \approx \times \left(\delta_{\alpha\beta} - \frac{\tau}{\gamma}u_{\alpha\beta}(\mathbf{r}_l) - \frac{\tau}{\gamma}\sum_{k\neq l} w_{\alpha\beta}(\mathbf{r}_l - \mathbf{r}_k)\right)\delta_{ln},$$

where $u_{\alpha\beta} \equiv \frac{\partial^2 u(\mathbf{r})}{\partial r_\alpha \partial r_\beta}$ and $w_{\alpha\beta} \equiv \frac{\partial^2 w(\mathbf{r})}{\partial r_\alpha \partial r_\beta}$. Substituting this approximation in Equation (15), we get

$$T_s \sum_\beta \frac{\partial}{\partial r_{\beta 1}}\Big[P_N^{(1)}(\mathbf{r}_1)\delta_{\alpha\beta} - \frac{\tau}{\gamma}P_N^{(1)}(\mathbf{r}_1)u_{\alpha\beta}(\mathbf{r}_1) - (N-1)\frac{\tau}{\gamma}\int \sum_k d\mathbf{r}_2 P_N^{(2)}(\mathbf{r}_1, \mathbf{r}_2) w_{\alpha\beta}(\mathbf{r}_1 - \mathbf{r}_2)\Big] = -P_N^{(1)}(\mathbf{r}_1)\frac{\partial u(\mathbf{r}_1)}{\partial r_{\alpha 1}} - (N-1) \times \int d\mathbf{r}_2 P_N^{(2)}(\mathbf{r}_1, \mathbf{r}_2)\frac{\partial w(\mathbf{r}_1 - \mathbf{r}_2)}{\partial r_{\alpha 1}}. \tag{16}$$

Such an equation, once a prescription for $P_N^{(2)}(\mathbf{r}_1, \mathbf{r}_2)$ is specified, can be used to derive the density profile of a system of interacting particles under inhomogeneous conditions. Let us remark that Equation (16) expresses the condition of mechanical equilibrium equivalent to the first member of the BBGY hierarchy as discussed in [21].

3. Effective potential

Let us apply Equation (11) to a system a system comprising just two particles so that the equation becomes closed:

$$T_s \sum_{\beta=1}^{d}\sum_{n=1}^{2} \frac{\partial}{\partial r_{\beta n}}[\Gamma^{-1}_{\alpha 1,\beta n}(\mathbf{r}_1, \mathbf{r}_2) P_2^{(2)}(\mathbf{r}_1, \mathbf{r}_2)] = -P_2^{(2)}(\mathbf{r}_1, \mathbf{r}_2)\left(\frac{\partial u(\mathbf{r}_1)}{\partial r_{\alpha 1}} + \frac{\partial w(\mathbf{r}_1 - \mathbf{r}_2)}{\partial r_{\alpha 1}}\right). \tag{17}$$

The solution is

$$P_2^{(2)}(\mathbf{r}_1, \mathbf{r}_2) = \frac{1}{Z_2}\exp\left(-\frac{\psi(\mathbf{r}_1, \mathbf{r}_2) + \frac{\tau}{2\gamma}\sum_{\alpha=1}^{d}[\frac{\partial}{\partial r_\alpha}\psi(\mathbf{r}_1, \mathbf{r}_2)]^2 - D\gamma \ln\det\Gamma(\mathbf{r}_1, \mathbf{r}_2)}{T_s}\right), \tag{18}$$

where $\psi(\mathbf{r}_1, \mathbf{r}_2) = u(\mathbf{r}_1) + u(\mathbf{r}_2) + w(\mathbf{r}_1 - \mathbf{r}_2)$ and $\det\Gamma$ is the determinant associated with the $2d \times 2d$ matrix whose elements are

$$\Gamma_{\alpha\beta}(\mathbf{r}_i, \mathbf{r}_j) = \delta_{\alpha\beta}\delta_{ij} + \frac{\tau}{\gamma}\frac{\partial^2\psi(\mathbf{r}_i, \mathbf{r}_j)}{\partial r_{\alpha i}\partial r_{\beta j}} \tag{19}$$

with $i, j = 1, 2$. The form of Equation (18) suggests the idea of introducing an effective potential to describe the interaction experienced by the particles when subjected to coloured noise. The effective potential can simplify the description, make the analysis more transparent and avoid the difficulty of evaluating the inverse matrix Γ when the system comprises a large number of particles. However, we must explore the validity of such a method since it involves an approximate treatment of the interactions when $N \geq 3$. Let us begin with the simplest case of just two particles free to move on a line in the absence of external fields and write the pair distribution. To this purpose, let us consider the 2×2 matrix Γ_{ij}:

$$\Gamma^{(2)} = \begin{pmatrix} 1 + \frac{\tau}{\gamma}w_{11}(x_1 - x_2) & -\frac{\tau}{\gamma}w_{11}(x_1 - x_2) \\ -\frac{\tau}{\gamma}w_{11}(x_1 - x_2) & 1 + \frac{\tau}{\gamma}w_{11}(x_1 - x_2) \end{pmatrix}$$

with $w_{11} = \frac{d^2 w(x_1 - x_2)}{dx_1^2}$. The resulting two particles distribution function $P_2^{(2)}$ has the form

$$P_2^{(2)}(x_1 - x_2) = \frac{1}{Z_2}\exp\left(-\frac{\phi(x_2 - x_1)}{T_s}\right). \tag{20}$$

Thus, we can define, apart from a constant, the following pair effective potential by taking the logarithm of P_2

$$\phi(x_1 - x_2) = w(x_1 - x_2) + \left(\frac{\tau}{\gamma}\right)[w_1(x_1 - x_2)]^2 - D\gamma \ln(1 + 2\left(\frac{\tau}{\gamma}\right)w_{11}(x_1 - x_2)) \tag{21}$$

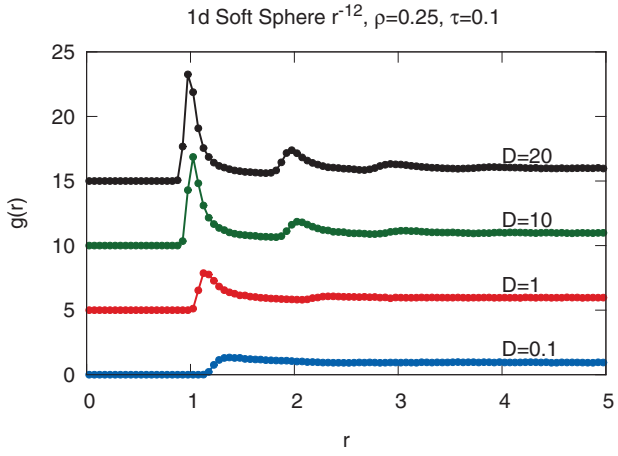

Figure 1. Results for the pair correlation function obtained via numerical simulation of a one-dimensional system. Density ρ is expressed in units σ^{-1}, τ in units γ^{-1} and D in units T_s/γ.

with $w_1 = \frac{dw(x_1-x_2)}{dx_1}$.

The above result can be generalised in the case of higher dimensionality. The pair correlation function in d dimensions for a two-particle system interacting via a central potential $w(r)$, in the absence of external potentials, reads

$$g(r) = \exp\left(-\frac{w(r) + \frac{\tau}{\gamma}[w'(r)]^2 - T_s \ln[(1+2\frac{\tau}{\gamma}w''(r))(1+2\frac{\tau}{\gamma}\frac{w'(r)}{r})^{d-1}]}{T_s}\right), \tag{22}$$

where the prime mean derivative with respect to the separation r. Thus, the effective pair potential reads $\phi(r) = -T_s \ln g(r)$. Let us remark that the effective potential, being derived in the low-density limit, does not account for the three-body terms which instead are present if one considers formula (12) with $N > 2$.

In all these cases, the dependence of ϕ on the effective temperature is quite interesting because as D increases, the effective potential displays a deeper and deeper potential well. Hereafter, we shall adopt the following unit system: lengths are expressed in terms of the molecular length σ, time in terms of the unit time γ^{-1} and the unit mass is set equal to 1.

In particular, we find that for a pair potential $w(x) = w_0(\frac{\sigma}{x})^{12}$, in order to observe an attractive region, it is necessary to have $2D\tau/\sigma^2 > 1$. This is shown in Figure 1 where we display the pair correlation function obtained by numerical simulations of a system of repulsive particles in one dimension for different values of D, average density $\rho\sigma = 0.25$ and for $\tau = 0.1$. The various curves correspond to different values of D and one can see that the height of the peak increases with D because the effective attraction increases. Such an effective attraction in a system where only repulsive inter-particle forces are in action is due to a dynamical mechanism. It can be understood as follows: the friction that a particle experiences with the background fluid is enhanced by the presence of surrounding particles so that their mobility decreases. Being less mobile, the particle tends to spend more time in configurations where it is closer to other particles and one interprets this situation as an effective attraction [12,28,29].

In spite of the fact that the MUCNA N-particle distribution function is known, it is difficult to apply it to large systems because of the many-body nature of the interactions. On the other hand, if one could replace the complicated MUCNA potential by an effective pairwise potential, it would possible to use all the machinery employed in the study of molecular fluids. Under this hypothesis, one could, for instance, use methods such as the density functional method, define a Helmholtz intrinsic free energy, or utilise the integral equations method and greatly simplify the study the phase behaviour of the model. To analyse its validity, we use a simple example: consider an interacting two-particle system subjected to the action of an external potential $u(x)$ whose distribution function is given by

$$P_2^{(2)}(x_1,x_2) = \frac{1}{Z_2}\exp\left(-\frac{w(x_1,x_2)+u(x_1)+u(x_2)}{T_s}\right) \times \exp\left(-\frac{\tau}{2\gamma T_s}\left[\frac{\partial}{\partial x_1}(w(x_1,x_2)+u(x_1))\right]^2 - \frac{\tau}{2\gamma T_s}\left[\frac{\partial}{\partial x_2}(w(x_1,x_2)+u(x_2))\right]^2 + \ln\det\Gamma(x_1,x_2)\right) \tag{23}$$

with

$$\det\Gamma(x_1,x_2) = 1 + \frac{\tau}{\gamma}\left(2\frac{\partial^2 w(x_1,x_2)}{\partial x_1^2} + \frac{\partial^2 u(x_1)}{\partial x_1^2} + \frac{\partial^2 u(x_2)}{\partial x_2^2}\right) + \left(\frac{\tau}{\gamma}\right)^2\left(\frac{\partial^2 w(x_1,x_2)}{\partial x_1^2}\left[\frac{\partial^2 u(x_1)}{\partial x_1^2} + \frac{\partial^2 u(x_2)}{\partial x_2^2}\right] + \frac{\partial^2 u(x_1)}{\partial x_1^2}\frac{\partial^2 u(x_2)}{\partial x_2^2}\right). \tag{24}$$

In the spirit of the effective potential idea, we introduce the following superposition approximation:

$$P_2^{approx}(x_1,x_2) \approx \frac{1}{Z_2^{approx}} \times \exp\left(-\frac{w(x_1,x_2)+u(x_1)+u(x_2)}{T_s}\right)$$

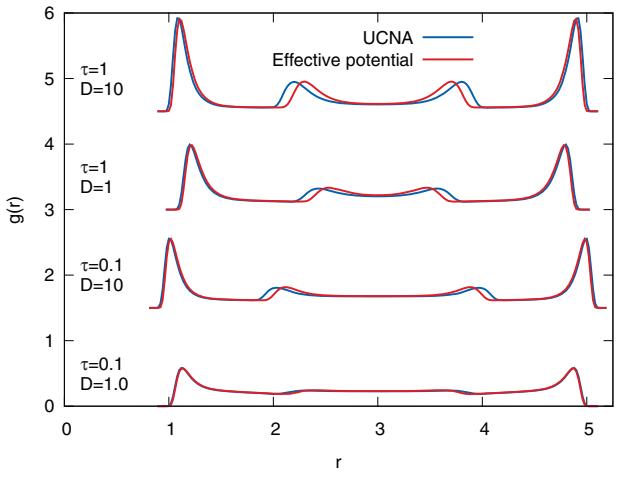

Figure 2. Normalised single-particle probability distribution function for a one-dimensional system with two interacting particles confined between two repulsive walls at $x = 0$ and $x = 6$. The wall repulsive potential is $u(x) = u_0(\frac{\sigma}{x})^{12}$ at each wall and $w(x_1 - x_2) = w_0(\frac{\sigma}{(x_1-x_2)})^{12}$ between the particles with $u_0 = w_0 = 1$. The curves refer to $\tau = 0.1, 1.$ and $D = 1, 10$ expressed in the same units as in Figure 1. The agreement between the Gaussian coloured noise result and the effective potential is poor as far as the second peak is concerned: its position is shifted towards larger distances from the wall, when the persistence time increases.

$$\times \exp\left(-\frac{\tau}{2\gamma T_s}\left[\frac{\partial}{\partial x_1} w(x_1, x_2)\right]^2 - \frac{\tau}{2\gamma T_s}\left[\frac{\partial}{\partial x_2} w(x_1, x_2)\right]^2 - \frac{\tau}{2\gamma T_s}\left[\frac{\partial}{\partial x_1} u(x_1)\right]^2 - \frac{\tau}{2\gamma T_s}\left[\frac{\partial}{\partial x_2} u(x_2)\right]^2 + \ln\det \Gamma^{approx}(x_1, x_2)\right) \quad (25)$$

with

$$\ln\det \Gamma^{approx}(x_1, x_2) \approx \ln\left(1 + 2\left(\frac{\tau}{\gamma}\right)\frac{\partial^2 w(x_1, x_2)}{\partial x_1^2}\right) + \ln\left(1 + \left(\frac{\tau}{\gamma}\right)\frac{\partial^2 u(x_1)}{\partial x_1^2}\right) + \ln\left(1 + \left(\frac{\tau}{\gamma}\right)\frac{\partial^2 u(x_2)}{\partial x_2^2}\right). \quad (26)$$

Clearly, the exact formula and the approximation for the determinant differ beyond the linear order in τ/γ, but perhaps the largest discrepancy occurs in the presence of cross terms of linear order in τ/γ, such as $w(x_1, x_2)u(x_1)$ in the interaction potential. A test can be performed by comparing the probability density profile $P^{(1)}(x_1)$ obtained by integrating over the coordinate x_2 the exact distribution and the one obtained by applying the same procedure to the approximate distribution (25). The comparison, displayed in Figure 2, reveals the presence of a systematic shift of the second peak of the approximate distribution towards larger distances from the confining wall, as if the total effective force were more repulsive.

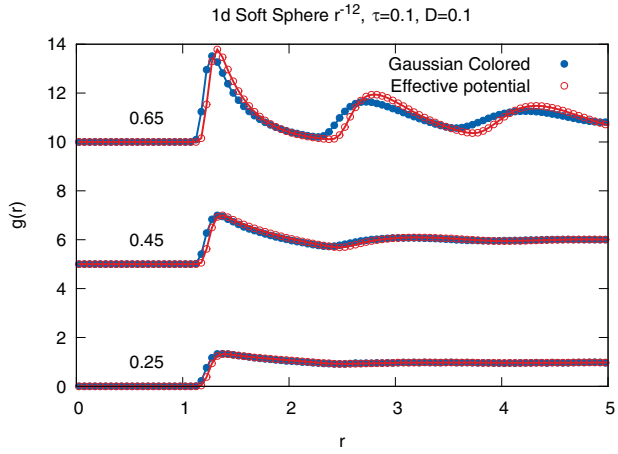

Figure 3. Numerical simulation of a one-dimensional system. Pair correlation for $\rho\sigma = 0.25, 0.45, 0.65$ for fixed $\tau = 0.1$ and $D = 0.1$, expressed in the same units as in Figure 1. The height of the peak increases with density. The agreement between the Gaussian coloured noise result and the effective potential is moderately good.

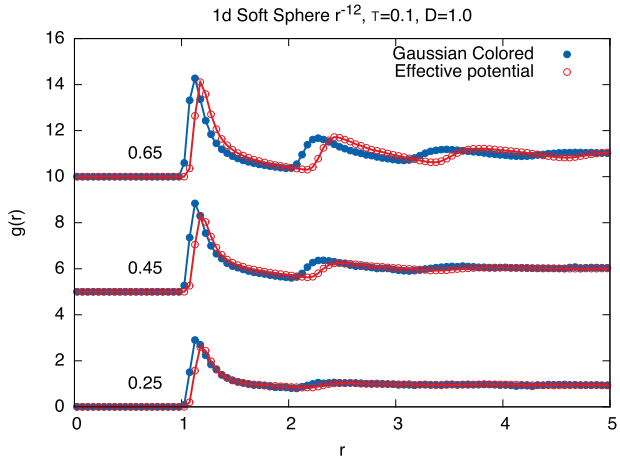

Figure 4. Numerical simulation of a one-dimensional system. Pair correlation for $\rho\sigma = 0.25, 0.45, 0.65$ for fixed $\tau = 0.1$ and $D = 1$, expressed in the same units as in Figure 1. The agreement between the Gaussian coloured noise result and the effective potential is rather poor due to the relatively large value of the persistence time.

We turn, now, to consider a many-particle systems and perform a similar comparison. We have simulated the system described by Equations (3) and (4) with $N = 1000$ and computed numerically the pair correlation function. In order to check the effective potential approximation, we also performed simulations of the over-damped Langevin equation with white noise for particles in one dimension subjected to interactions given by $\phi(x_i - x_j)$. The corresponding results are shown in Figures 3–6. One observes in Figures 3 and 4 that at moderately low

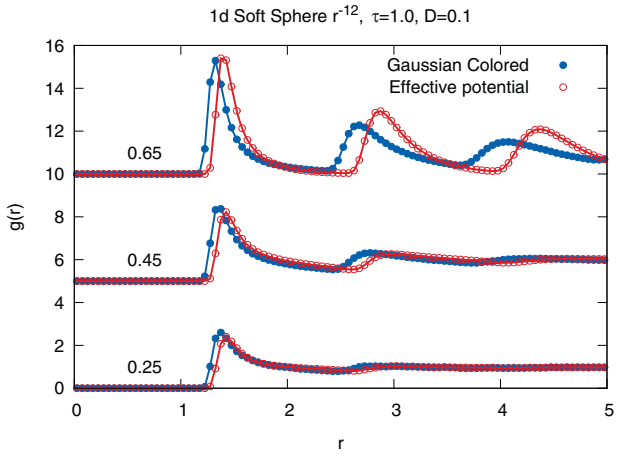

Figure 5. Numerical simulation of a one-dimensional system. Pair correlation for $\rho\sigma = 0.25, 0.45, 0.65$ for fixed $\tau = 1.$ and $D = 0.1$. The agreement between the Gaussian coloured noise result and the effective potential is rather poor due to the relatively large value of the persistence time.

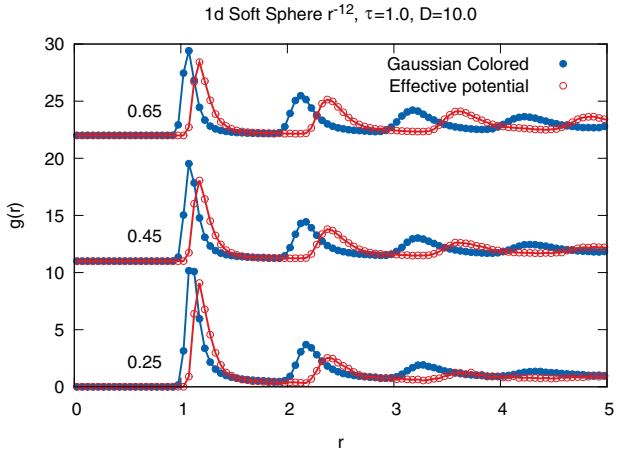

Figure 6. Numerical simulation of a one-dimensional system. Pair correlation for $\rho\sigma = 0.25, 0.45, 0.65$ for fixed $\tau = 1.$ and $D = 10$. The agreement between the Gaussian coloured noise result and the effective potential is rather poor due to the relatively large value of the persistence time.

values of the persistence time, $\tau = 0.1$, the discrepancy between the effective potential approximation and the full coloured noise result is not too large even at large densities, although there is a systematic shift of the peaks in the effective potential towards larger values of the distance. The situation at values of τ ten times larger, $\tau = 1$, and $D = 0.1$ and 10, is remarkably worse and the peaks of the effective theory display a much larger shift as illustrated by Figures 5 and 6. Such a shift is determined by the approximate treatment of the three-body repulsive term which appears in Equation (13) which becomes more relevant as the density and τ increase. These findings pose some limits to the possibility of obtaining reliable results by employing the effective potential approximation for values of the persistence time too large.

3.1. Van der Waals free energy

We use, now, a van der Waals (vdW) argument to estimate the free energy for the present model in d-dimension when the bare potential is of the form $w(r) = w_0(\frac{\sigma}{r})^\alpha$ and identify the following repulsive contribution in the effective potential:

$$\phi_{rep}(\tilde{r}) = w_0(\frac{\sigma}{r})^\alpha + \frac{\tau}{\gamma}\frac{\alpha^2}{\sigma^2}w_0^2(\frac{\sigma}{r})^{2\alpha+2}, \tag{27}$$

whereas, the attractive contribution is

$$\phi_{attr}(r) = -T_s \ln\left(\left[1 + 2\alpha(\alpha+1)\frac{w_0\tau}{\gamma\sigma^2}\left(\frac{\sigma}{r}\right)^{\alpha+2}\right] \times \left[1 - 2\alpha\frac{w_0\tau}{\gamma\sigma^2}\left(\frac{\sigma}{r}\right)^{\alpha+2}\right]^{d-1}\right). \tag{28}$$

Thus, for $w_0\frac{\tau}{\gamma\sigma^2} << 1$, the system reduces to a system of passive soft repulsive spheres. Using a standard procedure, we represent the free energy as the sum of a repulsive contribution evaluated in the local density approximation plus a non-local mean-field attractive term:

$$\mathcal{F}[\rho^{(1)}] = T_s\int d^dr\rho(\mathbf{r})\left[\ln\left(\frac{\rho^{(1)}(\mathbf{r})}{1-b\rho^{(1)}(\mathbf{r})}\right) - 1\right] + \frac{1}{2}\iint_{|\mathbf{r}-\mathbf{r}'|>R_b} d^dr d^dr'\,\phi_{attr}(\mathbf{r}-\mathbf{r}')\rho^{(1)}(\mathbf{r})\rho(\mathbf{r}'), \tag{29}$$

where $b = \omega_d R^d$, $\omega_d = 1, \pi/2, 2\pi/3$ for $d = 1, 2, 3$, respectively, and the effective hard-sphere diameter, R_b, is given by the Barker–Henderson formula:

$$R_b = \int_0^\infty dr(1 - e^{-\phi_{rep}(\tilde{r})/T_s}). \tag{30}$$

Following the standard vdW approach, we may represent the pressure associated with the functional (29) as

$$p = \frac{T_s\,\rho}{1-b\rho} - a\rho^2, \tag{31}$$

where the value of the coefficient a is determined by the strength of the effective attractive interaction

$$a = -\int_{R_b}^\infty d^dr\,\phi_{attr}(r). \tag{32}$$

From the form of the effective attractive potential (28), one sees that a is an increasing function of the non-dimensional parameter $\frac{w_0\tau}{\gamma\sigma^2}$ and of T_s. The latter feature determines a remarkable difference with respect to passive fluids: in that case, the vdW pressure is the sum of an entropic term proportional to the temperature and of

a negative temperature-independent enthalpic term. In active fluids, on the contrary, the coefficient a increases roughly linearly with T_s as the entropic term does. As a result, T_s, since a/T_s is nearly constant, does not play a major role in determining the critical parameters of the active model. The effective attraction among the particles has its origin in the reduction of their mobility, reflected by the presence of an effective friction Γ_{ij} in (7), which increases with increasing density. As a result, the particles tend to accumulate where their density is higher and move more slowly, and possibly lead to the mobility-induced phase separation phenomenon.

In analogy with the vdW model of passive fluids, one can determine the critical parameters, where a second-order transition would take place, by solving simultaneously the equations $\frac{\partial p}{\partial V} = 0$ and $\frac{\partial^2 P}{\partial V^2} = 0$ with the result

$$\frac{a(\tau_c)}{T_s} = \frac{27}{8} b\,, \qquad \rho_c = \frac{1}{3b}. \tag{33}$$

Thus, in order to have phase separation, the persistence time, τ, must exceed the critical value τ_c, implicitly given by the first part of Equation (33). However, the numerical investigation of the phase separation of Gaussian-coloured noise-driven particles is still in progress and so far it has not revealed a clear phase separation in the absence of attraction.

4. Conclusions

We discussed the properties of a newly introduced model describing an active fluid, consisting of an an assembly of repulsive soft spheres subject to over-damped dynamics and driven by a coloured noise. Although, within the MUCNA, it is possible to get an analytical expression for the many-particle distribution function, it is difficult to make progress without resorting to approximations. The effective potential hypothesis represents a practical possibility since it reduces the many-body potential to a pairwise additive potential where one can use the standard tools of statistical mechanics. To test the hypothesis, we performed two checks. In the first one, we employed a toy model consisting of just two particles in an external field and performed explicitly the analytic calculations. In the second check, we compared by numerical Brownian simulation the properties of a one-dimensional system of soft repulsive spheres subjected to coloured noise against the corresponding properties of a system of particles interacting via the effective potential. It is found that for values of the persistence time not too large, the effective potential approximation is reliable.

Disclosure statement

No potential conflict of interest was reported by the authors.

Funding

Claudio Maggi was supported by the European Research Council under the European Union's Seventh Framework programme [FP7/2007-2013], [ERC grant agreement number 307940]; Matteo Paoluzzi was supported by a grant [NSF-DMR-1305184].

References

[1] C. Bechinger, R. Di Leonardo, H. Lowen, C. Reichhardt, G. Volpe, and G. Volpe, ArXiv preprint arXiv:1602.00081 (2016).
[2] M. Marchetti, J. Joanny, S. Ramaswamy, T. Liverpool, J. Prost, M. Rao, and R.A. Simha, Rev. Mod. Phys. **85**(3), 1143–1189 (2013).
[3] M.C. Marchetti, Y. Fily, S. Henkes, A. Patch, and D. Yllanes, arXiv preprint arXiv:1510.00425 (2015).
[4] W. Poon, in *Proceedings of the International School of Physics Enrico Fermi, Course CLXXXIV Physics of Complex Colloids*, edited by C. Bechinger, F. Sciortino, and P. Ziherl (IOS, Amsterdam, 2013), pp. 317–386.
[5] P. Romanczuk, M. Baer, W. Ebeling, B. Lindner, and L. Schimansky-Geier, Eur. Phys. J. Spec. Top. **202**(1), 1–162 (2012).
[6] J. Elgeti, R.G. Winkler, and G. Gompper, arXiv preprint arXiv:1412.2692 (2014).
[7] M. Cates, Rep. Prog. Phys. **75**(4), 042601–042614 (2012).
[8] J. Bialké, H. Löwen, and T. Speck, arXiv preprint arXiv:1412.4601 (2014).
[9] Y. Fily and M.C. Marchetti, Phys. Rev. Lett. **108**(23), 235702–235706 (2012).
[10] J. Stenhammar, A. Tiribocchi, R.J. Allen, D. Marenduzzo, and M.E. Cates, Phys. Rev. Lett. **111**(14), 145702–145706 (2013).
[11] J. Tailleur and M. Cates, Phys. Rev. Lett. **100**(21), 218103–218106 (2008).
[12] M. Cates and J. Tailleur, Europhys. Lett. **101**(2), 20010–20015 (2013).
[13] H.C. Berg, *E. coli in Motion* (Springer Verlag, New York, 2004).
[14] M.J. Schnitzer, Phys. Rev. E **48**(4), 2553–2568 (1993).
[15] X. Zheng, B. ten Hagen, A. Kaiser, M. Wu, H. Cui, Z. Silber-Li, and H. Löwen, Phys. Rev. E **88**(3), 032304–032314 (2013).
[16] C. Maggi, M. Paoluzzi, N. Pellicciotta, A. Lepore, L. Angelani, and R. Di Leonardo, Phys. Rev. Lett. **113**(23), 238303–238307 (2014).
[17] N. Koumakis, C. Maggi, and R. Di Leonardo, Soft Matter **10**(31), 5695–5701 (2014).
[18] N. Koumakis, A. Lepore, C. Maggi, and R. Di Leonardo, Nat. Commun. **4** (2013).
[19] L. Angelani, C. Maggi, M. Bernardini, A. Rizzo, and R. Di Leonardo, Phys. Rev. Lett. **107**(13), 138302–138305 (2011).
[20] T. Farage, P. Krinninger, and J. Brader, Phys. Rev. E **91**(4), 042310–042319 (2015).

[21] U.M.B. Marconi and C. Maggi, Soft Matter **11**(45), 8768–8781 (2015).
[22] U.M.B. Marconi and S. Melchionna, J. Phys. Condens. Matter **22**(36), 364110–364117 (2010).
[23] P. Hanggi and P. Jung, Adv. Chem. Phys. **89**, 239 (1995).
[24] L. Cao, D.J. Wu, and X.L. Luo, Phys. Rev. A **47**(1), 57–70 (1993).
[25] C. Maggi, U.M.B. Marconi, N. Gnan, and R. Di Leonardo, Sci. Rep. **5** (2015).
[26] U.M.B. Marconi, N. Gnan, C. Maggi, M. Paoluzzi, and R. Di Leonardo, arXiv preprint arXiv:1512.04227 (2015).
[27] E.M. Purcell, Am. J. Phys. **45**(1), 3–11 (1977).
[28] M. Cates and J. Tailleur, Ann. Rev. Condens. Matter Phys. **6**(6), 219–244 (2015).
[29] J. Barré, R. Chétrite, M. Muratori, and F. Peruani, arXiv preprint arXiv:1403.2364 (2014).
[30] U.M.B. Marconi and P. Tarazona, J. Chem. Phys. **124**(16), 164901–164911 (2006).
[31] U. Marini-Bettolo-Marconi, P. Tarazona, and F. Cecconi, J. Chem. Phys. **126**, 164904 (2007).

Appendix A. Derivation of the UCNA equation by multiple time-scale analysis

In this appendix, we derive the UCNA approximation by a multiple time-scale analysis following the same method employed in [30,31]. It allows to derive in a systematic fashion the configurational Smoluchowski equation from the Kramers' equation via the elimination of the velocity degrees of freedom. To achieve this goal, one introduces fast and slow time-scale variables for the independent variable, and subsequently treats these variables, fast and slow, as if they are independent. The solution is first expressed as a function of these different time scales and subsequently these new independent variables are used to remove secular terms in the resulting perturbation theory. Physically speaking, the fast scale corresponds to the time interval necessary to the velocities of the particles to relax to configurations consistent with the values imposed by the vanishing of the currents. The slow time scale is much longer and corresponds to the time necessary to the positions of the particles to relax towards the stationary configuration.

It is convenient to work with non-dimensional quantities and introduce the following variables:

$$\bar{t} \equiv t\frac{v_T}{l}, \qquad V \equiv \frac{v}{v_T}, \qquad X \equiv \frac{x}{l},$$
$$\Gamma = \gamma\frac{l}{v_T}, \qquad \zeta = \frac{l}{\tau v_T} \tag{A1}$$
$$K(X) \equiv \frac{lF(x)}{mv_T^2}, \qquad v_T = \sqrt{D/\tau}, \tag{A2}$$

where l is a typical length of the problem, such as the size of the particles and ζ plays the role of a non-dimensional friction.

It is clear that if $\zeta \gg 1$ particles lose memory of their initial velocities after a time span which is of the order of the time constant τ so that the velocity distribution soon becomes stationary. We shall assume that $\gamma\tau$ stays finite when $\tau \to 0$. In this limit, the Smoluchowski description of a system of non-interacting particles, which takes into account only the configurational degrees of freedom, turns out to be adequate. However, for intermediate values of τ, the velocity may play a role. The question is how do we recover the UCNA starting from a description in the larger space x, v ? We rewrite Kramers' evolution equation for the phase-space distribution function using (A1) and (A2) as

$$\frac{\partial\tilde{f}(X,V,\bar{t})}{\partial\bar{t}} + V\frac{\partial}{\partial X}\tilde{f}(X,V,\bar{t}) + \frac{\zeta}{\Gamma}K(X,\bar{t})\frac{\partial}{\partial V}\tilde{f}(X,V,\bar{t}) = \zeta L_{FP}\tilde{f}(X,V,\bar{t}) \tag{A3}$$

having introduced the 'Fokker–Planck' operator

$$L_{FP}\tilde{f}(X,V,\bar{t}) = \frac{\partial}{\partial V}\Big[\frac{\partial}{\partial V} + s(X)V\Big]\tilde{f}(X,V,\bar{t}) \tag{A4}$$

with

$$s(X) = 1 - \frac{1}{\Gamma\zeta}\frac{dK}{dX}$$

whose eigenfunctions are

$$H_\nu(X,V) = (-1)^\nu\frac{1}{\sqrt{2\pi}}s^{-(\nu-1)/2}\frac{\partial^\nu}{\partial V^\nu}\exp\left(-\frac{s(X)}{2}V^2\right)$$

and have non positive eigenvalues $\nu = 0, -s, -2s, \ldots, -\nu s$. Note that, as stated above, we treat ζ/Γ as a quantity of order 1. Solutions of Eq.(A3), where the velocity dependence of the distribution function is separated, can be written as

$$\tilde{f}(X,V,\bar{t}) \equiv \sum_{\nu=0}^{\infty}\phi_\nu(X,\bar{t})H_\nu(X,V). \tag{A5}$$

In the multiple time-scale analysis, one determines the temporal evolution of the distribution function $\tilde{f}(X,V,\bar{t})$ in the regime $\zeta \gg 1$, by means of a perturbative method. In order to construct the solution, one replaces the single physical time scale, $\bar{t}$, by a series of auxiliary time scales $(\bar{t}_0, \bar{t}_1, \ldots, \bar{t}_n)$ which are related to the original variable by the relations $\bar{t}_n = \zeta^{-n}\bar{t}$. Also, the original time-dependent function, $\tilde{f}(X,V,\bar{t})$, is replaced by

an auxiliary function, $\tilde{f}_a(X, V, \bar{t}_0, \bar{t}_1, \ldots)$, that depends on the $\bar{t}_n$, treated as independent variables. Once the equations corresponding to the various orders have been determined, one returns to the original time variable and to the original distribution.

One begins by replacing the time derivative with respect to $\bar{t}$ by a sum of partial derivatives:

$$\frac{\partial}{\partial \bar{t}} = \frac{\partial}{\partial \bar{t}_0} + \frac{1}{\zeta}\frac{\partial}{\partial \bar{t}_1} + \frac{1}{\zeta^2}\frac{\partial}{\partial \bar{t}_2} + \cdots \tag{A6}$$

First, the function, $\tilde{P}(X, V, \bar{t}_0, \bar{t}_1, \ldots)$ is expanded as a series of ζ^{-1}

$$\tilde{P}\left(X, V, \bar{t}_0, \bar{t}_1, \bar{t}_2, \ldots\right) = \sum_{s=0}^{\infty} \frac{1}{\zeta^s} \sum_{\nu=0}^{\infty} \psi_{s\nu}\left(X, \bar{t}_0, \bar{t}_1, \bar{t}_2, \ldots\right) H_\nu(X, V) \tag{A7}$$

One substitutes, now, the time derivative (A6) and expression (A7) into Eq.(A3), and identifying terms of the same order in ζ^{-1} in the equations, one obtains a hierarchy of relations between the amplitudes $\psi_{s\nu}$. To order ζ^0, one finds:

$$L_{FP}\left[\sum_\nu \psi_{0\nu} H_\nu\right] = 0 \tag{A8}$$

and concludes that only the amplitude ψ_{00} is non-zero.

Next, we consider terms of order ζ^{-1} and write

$$L_{FP}\left[\psi_{11}H_1 + \psi_{12}H_2 + \psi_{13}H_3\right] = \frac{\partial \psi_{00}}{\partial \bar{t}_0} H_0 + \left(V\frac{\partial}{\partial X} + \frac{\zeta}{\Gamma}K(X, \bar{t})\frac{\partial}{\partial V}\right) H_0(X, V)\psi_{00}. \tag{A9}$$

After some straightforward calculations and equating the coefficients multiplying the same H_ν, we find

$$\frac{\partial \psi_{00}}{\partial \bar{t}_0} = 0 \tag{A10}$$

and

$$\psi_{11} = -s^{-3/2}\left(\frac{\partial}{\partial X} - \frac{s'}{s} - s\frac{\zeta}{\Gamma}K\right)\psi_{00}, \tag{A11}$$

where $s' = ds/dx$. According to (A10), the amplitude ψ_{00} is constant with respect to $\bar{t}_0$ and so is ψ_{11} being a functional of ψ_{00}. The remaining amplitudes $\psi_{1k} = 0$ are zero for all $k > 1$ with the exception of

$$\psi_{13} = \frac{1}{6}s^{-5/2}s'\psi_{00}. \tag{A12}$$

The equations of order ζ^{-2} give the conditions:

$$\frac{\partial \psi_{00}}{\partial \bar{t}_1} = -\frac{\partial}{\partial X}\left(\frac{\psi_{11}}{s^{1/2}}\right). \tag{A13}$$

If we truncate the expansion to second order and collect together the various terms and employing Eq. (A6) to restore the original time variable $\bar{t}$, we obtain the following evolution equation:

$$\frac{\partial \psi_{00}}{\partial \bar{t}} = \frac{1}{\zeta}\frac{\partial}{\partial X}\left[\frac{1}{s}\left(\frac{\partial}{\partial X}\left(\frac{\psi_{00}}{s}\right) - \frac{\zeta}{\Gamma}K\psi_{00}\right)\right]. \tag{A14}$$

Now, we can return to the original dimensional variables:

$$\frac{\partial P(x,t)}{\partial t} = D\frac{\partial}{\partial x}\left\{\frac{1}{1-\frac{\tau}{\gamma}F'(x)}\left[\frac{\partial}{\partial x}\left(\frac{P(x,t)}{1-\frac{\tau}{\gamma}F'(x)}\right) - \frac{1}{D\gamma}F(x)P(x,t)\right]\right\}. \tag{A15}$$

Equivalently, such a result would have followed by starting from the effective Langevin equation:

$$\frac{dx}{dt} = \frac{1}{\gamma}\frac{F(x)}{1-\frac{\tau}{\gamma}F'(x)} + \frac{D^{1/2}}{1-\frac{\tau}{\gamma}'(x)}\xi^w(t), \tag{A16}$$

which displays a space-dependent friction and a space-dependent noise.

Clearly, the stationary configurational distribution associated with (A15) is

$$P(x) = \mathcal{N}\left(1 + \frac{\tau}{\gamma}\frac{d^2u}{dx^2}\right) \times \exp\left[-\frac{1}{D\gamma}\left(u(x) + \frac{\tau}{2\gamma}\left(\frac{du}{dx}\right)^2\right)\right], \tag{A17}$$

where we introduced a normalisation factor.

Finally, since $P(x)$ is proportional to the amplitude of the H_0 mode, that is, the Maxwellian, we can write the following approximate steady-state phase-space distribution function, corresponding to the state with vanishing currents:

$$f(x, v) = \mathcal{N}\sqrt{\frac{\tau}{2\pi D}}\sqrt{\frac{1}{1-\tau F'(x)/\gamma}} \times \exp\left(\frac{1}{1-\tau F'(x)/\gamma}\frac{\tau}{D}v^2\right)P(x). \tag{A18}$$

Appendix B. Evaluation of the determinant for large *N*

The exact evaluation of the determinant of the matrix Γ and of its inverse is a formidable task and is far beyond the authors capabilities. However, it is possible to provide an approximate matrix inversion by expanding to linear order in τ/γ the formulas. In order to illustrate the point, we consider the matrix in the case of N particles in two spatial dimensions:

$$\begin{pmatrix} [1+\frac{\tau}{\gamma}\sum_{j\neq 1} w_{xx}(\mathbf{r}_1,\mathbf{r}_j)] & \sum_{j\neq 1}\frac{\tau}{\gamma} w_{xy}(\mathbf{r}_1,\mathbf{r}_j) & -\frac{\tau}{\gamma} w_{xx}(\mathbf{r}_1,\mathbf{r}_2) & \cdots & -\frac{\tau}{\gamma} w_{xy}(\mathbf{r}_1,\mathbf{r}_N) \\ \sum_{j\neq 1}\frac{\tau}{\gamma} w_{yx}(\mathbf{r}_1,\mathbf{r}_j) & [1+\frac{\tau}{\gamma}\sum_{j\neq 1} w_{yy}(\mathbf{r}_1,\mathbf{r}_j)] & -\frac{\tau}{\gamma} w_{yx}(\mathbf{r}_1,\mathbf{r}_2) & \cdots & -\frac{\tau}{\gamma} w_{yy}(\mathbf{r}_1,\mathbf{r}_N) \\ -\frac{\tau}{\gamma} w_{xx}(\mathbf{r}_2,\mathbf{r}_1) & -\frac{\tau}{\gamma} w_{yx}(\mathbf{r}_2,\mathbf{r}_1) & [1+\frac{\tau}{\gamma}\sum_{j\neq 2} w_{xx}(\mathbf{r}_2,\mathbf{r}_j)] & \cdots & -\frac{\tau}{\gamma} w_{xy}(\mathbf{r}_2,\mathbf{r}_N) \\ \cdots & \cdots & \cdots & \cdots & \cdots \\ -\frac{\tau}{\gamma} w_{xy}(\mathbf{r}_N,\mathbf{r}_1) & -\frac{\tau}{\gamma} w_{yy}(\mathbf{r}_N,\mathbf{r}_1) & \cdots & \cdots & [1+\frac{\tau}{\gamma}\sum_{j\neq N} w_{yy}(\mathbf{r}_N,\mathbf{r}_j)] \end{pmatrix}.$$

It is interesting to remark that the off-diagonal elements contain only one term, while the diagonal elements and their neighbours contain N elements. Thus, in the limit of $N\to\infty$, we expect that the matrix becomes effectively diagonal.

$$\begin{pmatrix} [1+\frac{\tau}{\gamma}\sum_{j\neq 1} w_{xx}(\mathbf{r}_1,\mathbf{r}_j)] & \sum_{j\neq 1}\frac{\tau}{\gamma} w_{xy}(\mathbf{r}_1,\mathbf{r}_j) & 0 & \cdots & 0 \\ \sum_{j\neq 1}\frac{\tau}{\gamma} w_{yx}(\mathbf{r}_1,\mathbf{r}_j) & [1+\frac{\tau}{\gamma}\sum_{j\neq 1} w_{yy}(\mathbf{r}_1,\mathbf{r}_j)] & 0 & \cdots & 0 \\ \cdots & \cdots & \cdots & \cdots & \cdots \\ 0 & 0 & 0 & [1+\frac{\tau}{\gamma}\sum_{j\neq N} w_{xx}(\mathbf{r}_N,\mathbf{r}_j)] & \sum_{j\neq 2}\frac{\tau}{\gamma} w_{yx}(\mathbf{r}_N,\mathbf{r}_j) \\ 0 & 0 & 0 & \sum_{j\neq N}\frac{\tau}{\gamma} w_{yx}(\mathbf{r}_N,\mathbf{r}_j) & [1+\frac{\tau}{\gamma}\sum_{j\neq N} w_{yy}(\mathbf{r}_N,\mathbf{r}_j)] \end{pmatrix}.$$

Its inverse is approximately

$$\begin{pmatrix} [1-\frac{\tau}{\gamma}\sum_{j\neq 1} w_{xx}(\mathbf{r}_1,\mathbf{r}_j)] & -\sum_{j\neq 1}\frac{\tau}{\gamma} w_{xy}(\mathbf{r}_1,\mathbf{r}_j) & 0 & \cdots & 0 \\ -\sum_{j\neq 1}\frac{\tau}{\gamma} w_{yx}(\mathbf{r}_1,\mathbf{r}_j) & [1-\frac{\tau}{\gamma}\sum_{j\neq 1} w_{yy}(\mathbf{r}_1,\mathbf{r}_j)] & 0 & \cdots & 0 \\ \cdots & \cdots & \cdots & \cdots & \cdots \\ 0 & 0 & 0 & [1-\frac{\tau}{\gamma}\sum_{j\neq N} w_{xx}(\mathbf{r}_N,\mathbf{r}_j)] & -\sum_{j\neq 2}\frac{\tau}{\gamma} w_{yx}(\mathbf{r}_N,\mathbf{r}_j) \\ 0 & 0 & 0 & -\sum_{j\neq N}\frac{\tau}{\gamma} w_{yx}(\mathbf{r}_N,\mathbf{r}_j) & [1-\frac{\tau}{\gamma}\sum_{j\neq N} w_{yy}(\mathbf{r}_N,\mathbf{r}_j)] \end{pmatrix}.$$

The determinant to order τ/γ is

$$\det\Gamma \approx 1+\frac{\tau}{\gamma}\sum_{i,j,i\neq j}[w_{xx}(\mathbf{r}_i,\mathbf{r}_j)+w_{yy}(\mathbf{r}_i,\mathbf{r}_j)]. \tag{B1}$$